Available online at www.sciencedirect.com
SCIENCE DIRECT®
Tetrahedron: Asymmetry
Tetrahedron: *Asymmetry* 15 (2004) 109–118

Synthesis and comparative study of the physicochemical properties of the related optically active complexes [(μ-H)Os_3{μ-OCNH-(*R*)-CHMePh}$(CO)_9$L]{L = CO, NMe_3, (*S*)-(–)-, or (*R*)-(+)-NH_2CHMePh}, toward the cluster and amino ligand configuration determination

Victoria A. Ershova,* Vladimir M. Pogrebnyak, Anatoly V. Golovin, Alexander V. Virovets and Peter P. Semyannikov

Nikolaev Institute of Inorganic Chemistry, Russian Academy of Sciences (RAS), Siberian Branch, Acad. Lavrentyev prosp. 3, Novosibirsk 630090, Russian Federation

Received 4 September 2003; accepted 14 November 2003

Abstract—A series of eight related optically active complexes having two or three stereogenic centers, [(μ-H)Os_3{μ-OCNH-(*R*)-CHMePh}$(CO)_{10}$], **1**, and [(μ-H)Os_3{μ-OCNH-(*R*)-CHMePh}$(CO)_9$L] {L = NMe_3, **2**, and (*S*)-(−)- or (*R*)-(+)-NH_2CHMePh, **3**}, have been prepared and characterized by ^{1}H and ^{13}C NMR, IR, mass-spectral, and $[\alpha]_D$ data. As shown by comparison of ^{1}H NMR spectra in the highly informative upfield region, the relative values of $\delta_{\mu\text{-H}}$ for corresponding diastereomers depend on a number of stereogenic centers in the molecule, the nature of L (CO or amine) and solvent and most of all on the absolute configuration of the cluster fragment [HOs_3(μ-OCN)]. The relative positions of hydride signals in ^{1}H NMR spectra of the diastereomeric pairs **1**–**3** correlates with the cluster-fragment configuration. The largest value of nonequivalence $\Delta\delta_{\mu\text{-H}}$ (0.36 ppm) was demonstrated by the diastereomers having the opposite cluster-fragment configurations and L = (*S*)-(−)-NH_2CHMePh in $CDCl_3$ solution.

1. Introduction

The chiral complexes [(μ-H)Os_3(μ-OCNR′R″)$(CO)_9$L] (R′ = H, alkyl; R″ = H, alkyl, aryl; L = CO or another 2-electron donor) containing a carboxamido bridging ligand represent an interesting class of model stereochemical objects due to the specific aspect that their chirality derives from the metal frame asymmetrically surrounded by ligands. In addition, they may also bear chiral R′, R″, or L substituents, and then they exist as a mixture of diastereomers. The first diastereomers of this type with L = CO, R′ = H, R″ = (*R*)- or (*S*)-CHMePh were obtained as two separated compounds by Arce and Deeming.[1] Later, the resolution of racemic complexes containing no chiral ligands into the enantiopure antipodes was developed in our laboratory.[2] However, the development of optically active compounds [(μ-H)Os_3(μ-OCNR′R″)$(CO)_9$L] has so far been limited because such metal complexes are expensive and difficult to resolve, and moreover, it is very difficult to grow satisfactory single crystals for X-ray diffraction.

Recently we initiated research concerning the action of the complexes [(μ-H)Os_3(μ-OCNR′R″)$(CO)_{10}$] as catalysts for the double-bond migration in *N*-allylic substrates.[3] Our efforts were focused on a development of this catalytic reaction as potentially enantioselective where the above complexes in their enantiomerically pure form would induce chirality during the course of the isomerization of a pro-chiral substrate. The plausible reaction mechanism involves maintaining a catalyzing cluster molecule configuration during the whole catalytic cycle.[4] This discovery is encouraging and stimulating extensive preparations of the optically active complexes [(μ-H)Os_3(μ-OCNR′R″)$(CO)_9$L] and the development of indirect methods allowing their chirality to be defined immediately from the reaction mixture analysis, in particular using NMR methods. It would give the important information as to whether retention of cluster configuration or racemization occurred. In the

* Corresponding author. Fax: +7-383-234-4489; e-mail: ersh@che.nsk.su

0957-4166/$ - see front matter © 2003 Elsevier Ltd. All rights reserved.
doi:10.1016/j.tetasy.2003.11.012

case when an enantiomeric cluster is used for the reaction (R′, R″, and L are achiral), it should be converted into corresponding diastereomeric derivatives by replacement of the achiral L by an optically active substituent. However, in reality such diastereomeric molecules show very little to no spectroscopic nonequivalence. ^{1}H NMR spectroscopic behavior of the above type of diastereomeric complexes has not been studied in detail until now, neither the sensitivity of the nonequivalence $\Delta\delta$ between diastereomers to the number of chiral centers in the cluster molecule, configuration of the cluster fragment, the nature of ligand L and solvent etc. This could be best achieved dealing with a sequence of related compounds with varying numbers of stereogenic centers and with configurations of both the cluster fragment [Os_3(μ-OCN)] and the bridging and terminal ligands being ascertained.

Additionally our interest concerns the possibility of developing the optically active clusters [(μ-H)Os_3(μ-OCNR′R″)$(CO)_{10}$] as analytical reagents for determining enantiomer composition and absolute configuration of a chiral molecule L, specifically when L is chiral amine, through the corresponding diastereomers [(μ-H)Os_3(μ-OCNR′R″)$(CO)_9$L]. In this context, the NMR spectroscopic study of (*R*)-amine substituted complexes in comparison with those of (*S*)-amine substituted complexes should give meaningful information. To our knowledge, no studies in this field have yet been performed with optically active clusters.

In this work, we report some empirical correlations between stereochemical features (the number of stereogenic centers, the cluster fragment [Os_3(μ-OCN)] and the terminal ligand configurations) and physicochemical properties of the eight related optically active complexes [(μ-H)Os_3{μ-OCNH-(*R*)-CHMePh}$(CO)_9$L] with (*R*)-α-phenylethylcarboxamido bridging ligand and L = CO **1**, NMe_3 **2**, and (*R*)- or (*S*)-NH_2CHMePh **3** (Fig. 1).

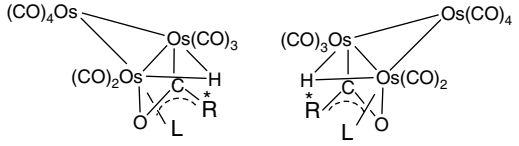

R* = (*R*)-NHC*HMePh;
L = CO **1**, NMe_3 **2**, (*R*)- or (*S*)-NH_2C*HMePh, **3**

Figure 1. Chiral molecules **1**–**3** considered in the study.

2. Results and discussion

The diastereomers [(μ-H)Os_3{μ-OCNH-(*R*)-CHMePh}-$(CO)_{10}$] (*a*,*R*)-**1** and (*b*,*R*)-**1** differing with *a* or *b* configuration of the cluster fragment [HOs_3(μ-OCN)] and having the same bridging (*R*)-α-phenylethylcarboxamido ligand have been obtained by the reaction of [$Os_3(CO)_{11}$NCMe] and (*R*)-(+)-α-phenylethylamine in THF at room temperature in the ratio (*a*,*R*)-**1**/(*b*,*R*)-**1**≈1:2 [(*b*,*R*)-**1** is the slower to elute on chromatography in any eluent)].[5] Previously these diastereomers have been already prepared from the [$Os_3(CO)_{12}$].[1] Subsequent reaction of (*a*,*R*)-**1** and (*b*,*R*)-**1** with Me_3NO in diethyl ether gave their optically active derivatives [(μ-H)Os_3{μ-OCNH-(*R*)-CHMePh}$(CO)_9(NMe_3)$] (*a*,*R*)-**2-NMe$_3$** and (*b*,*R*)-**2-NMe$_3$**, respectively, as orange solids. Reaction of the complexes (*a*,*R*)-**1** and (*b*,*R*)-**1** with (*R*)- or (*S*)-α-phenylethylamine in THF in the presence of Me_3NO leads to two pairs of the diastereomers, [(μ-H)Os_3{μ-OCNH-(*R*)-CHMePh}$(CO)_9${(*R*)-NH_2CHMePh}] and [(μ-H)Os_3{μ-OCNH-(*R*)-CHMePh} $(CO)_9$-{(*S*)-NH_2CHMePh}] (*a*,*R*,*R*)-**3**, (*b*,*R*,*R*)-**3** and (*a*,*R*,*S*)-**3**, (*b*,*R*,*S*)-**3**, respectively. Direct preparation from the unresolved mixture of (*a*,*R*)-**1** and (*b*,*R*)-**1** results in a mixture of the four diastereomers **3**, which could not be resolved into the individual species by chromatography. While the complexes **3** are moderately stable to air, moisture, and light (*a*-configurational complexes are less stable relative to *b*-configurational ones), the complexes **2** decompose smoothly, particularly in chlorinated hydrocarbon solutions, even when cold.

The compounds **1**–**3** obtained constitute a range of eight related optically active complexes, represented schematically in Figure 2. The IR, mass-spectral, ^{1}H and ^{13}C NMR data for these compounds are summarized in Table 1 and are in total accordance with their supposed structures and formulae. Mass-spectral data have shown that two complexes **1**, two complexes **2**, and four complexes **3** are isomeric within each group. While molecular ion peaks are detected only in the mass spectra of (*a*,*R*)-**1**, (*b*,*R*)-**1**, and (*b*,*R*)-**2-NMe$_3$** (M^+ 1005, 1005, and 1030 to ^{192}Os-peak) confirmation of the isomeric composition in each group complexes comes from an identity of the metal-containing ionic fragments and their different intensities indicating a different tendency of stereoisomers for the cleavage of corresponding bonds. Molecules **2** lose initially CH_3^+ and $MeC_2H_4^+$ ions followed by successive loss of nine CO groups. Molecules **3** lose $C_6H_5^+$ and $PhC_2H_4^+$ ions and then nine CO groups. In the spectra of **1** successive loss of 10 carbonyls have been also detected.

Comparison of the IR data for compounds **2** and **3** with those for structurally characterized complexes of a related nature suggests that amino ligands are coordinated equatorially to the oxygen-bonded Os atom.[6,7]

The four of these compounds (*a*,*R*)-**1**, (*b*,*R*)-**1**, (*a*,*R*)-**2-NMe$_3$** and (*b*,*R*)-**2-NMe$_3$** bear two stereogenic centers each and the four others (*a*,*R*,*R*)-**3**, (*b*,*R*,*R*)-**3**, and (*a*,*R*,*S*)-**3**, (*b*,*R*,*S*)-**3** have three stereogenic centers each. One stereogenic element resides on the cluster moiety [(μ-H)Os_3(μ-OCN)] and the two others localize in the bridging and terminal ligands. The alternative, *a* or *b*, configuration of the cluster moiety was ascribed to each complex in accordance with the absolute structure of one of these related complexes, (*b*,*R*)-**1**, determined earlier by single-crystal X-ray diffraction (Fig. 1).[5]

^{13}C and ^{13}C{^{1}H} NMR spectra have been registered for the stereoisomers **1**–**3** and their assignments were

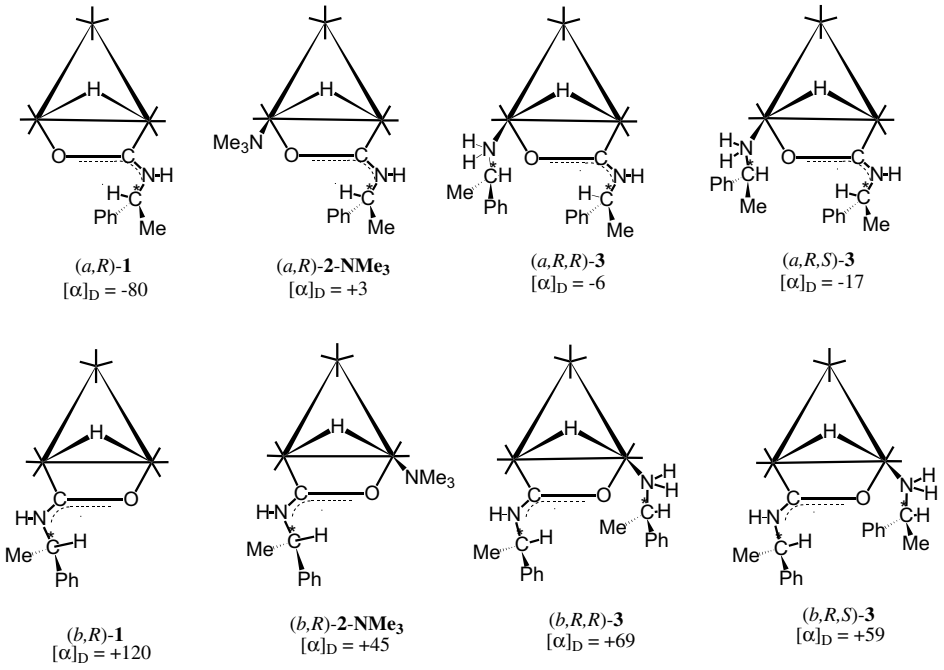

Figure 2. A series of eight related optically active complexes **1**–**3** bearing two or three stereogenic centers each and their $[\alpha]_D^{20}$ values (*c* 1, $CHCl_3$). The atom μ-H is nearest to the eye.

undertaken using the ^{13}C–^{1}H coupling constant values and the literature data for related ^{13}CO-enriched samples.[8] Separate signals from all CO groups are observed in the $^{13}C\{^{1}H\}$ spectra of complexes **1**–**3** (62.9 MHz, C_6D_6, room temperature) indicating that the molecules are stereochemically static on the NMR time scale and do not undergo racemization or epimerization. The unsubstituted complexes (*a*,*R*)-**1** and (*b*,*R*)-**1** contain in the carbonyl region of the spectra 11 discrete singlets each and their amino substituted derivatives **2** and **3** display 10 such signals each. The most downfield signal in each spectrum is unambiguously assigned to the carbonyl group of the bridging carboxamido ligand because of its splitting into doublet of doublets of doublets due to couplings with the neighboring μ-H, CH, and NH protons. This is in agreement with the published ^{13}C NMR data for bridging CO carbon in other related carboxamido and acyl complexes.[8,9] Comparison of the $^{13}C\{^{1}H_{NH}\}$ and $^{13}C\{^{1}H_{\mu\text{-}H}\}$ decoupled spectra of (*a*,*R*)-**1** has shown that $^{2}J_{CH}$ coupling constant (6.4–6.7 Hz) between μ-CO carbon and the amido NH proton is larger than $^{2}J_{CH}$ and $^{3}J_{CH}$ couplings (2.3–4 Hz) with μ-H and CH protons, respectively. An interesting feature is that the μ-CO signals in the spectra of (*a*,*R*)-**1**, (*a*,*R*)-**2-NMe$_3$**, (*a*,*R*,*R*)-**3**, and (*a*,*R*,*S*)-**3** (δ 184.5, 187.0, 186.0, 185.9) are shifted less downfield with respect to their *b*-configurational isomers (*b*,*R*)-**1**, (*b*,*R*)-**2-NMe$_3$**, (*b*,*R*,*R*)-**3**, and (*b*,*R*,*S*)-**3** (δ 184.9, 187.8, 186.6, 186.5). The μ-CO carbon atom is in a near to axial position with respect to Os_3 triangle (Fig. 3), and the same range of $^{2}J_{CH}$ is observed also for two other axial and also for two (complexes **1**) or one (complexes **2** and **3**) equatorial CO carbons at the bridged Os atoms. The change in a number of such terminal CO signals having *J* around 3–4 Hz from four for the unsubstituted (*a*,*R*)-**1** and (*b*,*R*)-**1** to three for the substituted **2** and **3** is consistent with the suggestion that amino ligand in **2** and **3** has occupied the equatorial position at the O-bonded Os. In each ^{13}C spectrum there are also two carbonyl carbon signals with larger $^{2}J_{CH}$ coupling constants (about 10–13 Hz) corresponding to two *trans*-to-μ-H CO ligands and four signals with very low $^{3}J_{CH}$ (0–1 Hz) corresponding to two axial and two equatorial CO carbon atoms on the top Os atom. Two of these four signals resonate at a lower field and were assigned to axial carbonyl carbons according to the literature data.[8] Signals from every carbon atom of the bridging and terminally bonded organic substituents are also found in the spectra and unambiguously assigned by their ^{1}H-splitting patterns.

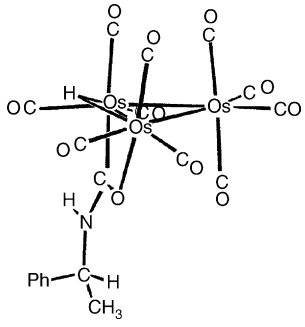

Figure 3. Schematic representation of the molecule absolute configuration for the (+)-rotating diastereomer, (*b*,*R*)-**1**.

Though the magnitude of the specific rotation depends on many factors and cannot be simply utilized for assignment of the configuration of any novel compound or other stereochemical details, it is still useful to compare the $[\alpha]_D$'s for the complexes **1**–**3** since they are related compounds. In Figure 2, we show the specific

rotation values measured under identical conditions (20 °C, $c = 1$, $CHCl_3$) for each of the optically active complexes **1**–**3**. The diastereomers (*a*,*R*)-**1** and (*b*,*R*)-**1** bearing the same (*R*) bridging ligand are opposite rotating with values −80 and 120, respectively. The rotation sign remains negative in going from (*a*,*R*)-**1** to its amino substituted derivatives (*a*,*R*,*R*)-**3** and (*a*,*R*,*S*)-**3**, just as the sign is positive for every *b*-configurational complex. It should be noted that the pair [(μ-H)Os_3{μ-OCNH-(*R*)-CHMePh}$(CO)_9$(NH_2CHMePh)], (*a*,*R*,*R*)-**3**/(*a*,*R*,*S*)-**3** or (*b*,*R*,*R*)-**3**/(*b*,*R*,*S*)-**3**, having identical (*a* or *b*, respectively) configurations of cluster fragment [(μ-H)Os_3(μ-OCN)] but opposite configurations, (*R*) or (*S*), of the terminal ligand exhibit closely-related $[\alpha]_D$ parameters, −6/−17 and +69/+59, respectively. Obviously, the cluster-fragment configuration plays the main role in the overall specific rotation of a cluster molecule compared to that of both bridging and terminal ligands. Moreover, an amino substituent as a pendant arm resulted in a positional shift of the molecular stereogenic center and alteration of the $[\alpha]_D$ values. This effect is even more evident in the case of the diastereomeric pair (*a*,*R*)-**2-NMe$_3$**/(*b*,*R*)-**2-NMe$_3$** containing the achiral NMe_3-substituent. Both derivatives became (+)-rotating +3/+45, respectively, without change in a number of stereogenic centers.

The complexes **1**, **2**, and **3** were characterized by infrared spectroscopy in the CO stretching region (Table 1). Close *ν*(CO) values are observed within the pairs both **1** and **3** with variation in frequencies of no more than 6 cm^{-1}.

The pair (*a*,*R*)-**2-NMe$_3$**/(*b*,*R*)-**2-NMe$_3$** differs to a greater extent, and the value of Δ*ν*(CO) for selected bands mounts to 10 cm^{-1}. This feature makes us suppose that the incoming amino substituent results not only in structural changes in a molecule, but also in larger structural differences between two diastereomers as compared to the parent **1**. A structural difference effected by the bulky NMe_3-ligand appears to be more significant than that caused by the chiral NH_2CHMePh-ligands. Unfortunately, an X-ray analysis of (*b*,*R*)-**2-NMe$_3$** and its structural comparison with (*b*,*R*)-**1** (Fig. 3) and (*a*,*R*)-**2-NMe$_3$** could not be performed because of the difficulty of growing an X-ray quality crystal of unstable complexes **2**.

The availability of ^{1}H NMR data for each of the diastereomers **1**–**3** is important not only in view of their identification by the NMR spectroscopy when they are in a mixture but also to reveal some correlations, if any, between spectroscopic data (mainly the separation of the chemical shifts, Δ*δ*, for corresponding protons in the diastereomeric pairs) and stereochemical features. The ^{1}H NMR spectra of the eight related complexes **1**–**3** in $CDCl_3$ are shown in Figure 4 together with the assignments.

In the aliphatic region, the values, Δ*δ*, for related protons within the diastereomeric pairs (*a*,*R*,*R*)-**3**/(*a*,*R*,*S*)-**3**, and (*b*,*R*,*R*)-**3**/(*b*,*R*,*S*)-**3** having opposite terminally bonded ligand configurations are not significant (see Table 1 and Fig. 4), whereas Δ*δ* is much larger for the same molecules grouped as (*a*,*R*,*R*)-**3**/(*b*,*R*,*R*)-**3** and (*a*,*R*,*S*)-**3**/(*b*,*R*,*S*)-**3**, having the opposite *a*/*b* cluster configurations (for instance, $\Delta\delta \approx 0.35$ and 0.3 ppm for CH_3 and α-CH protons of the terminally bonded ligands). For the other *a*/*b* pair, (*a*,*R*)-**2-NMe$_3$**/(*b*,*R*)-**2-NMe$_3$**, containing an achiral NMe_3 substituent, signals are also noticeably spaced (for instance, $\Delta\delta \approx 0.2$ and 0.52 ppm for α-CH and NMe_3 protons, respectively), and the 0.52 ppm value was registered to be the largest Δ*δ* value of all. The unsubstituted diastereomers (*a*,*R*)-**1**/

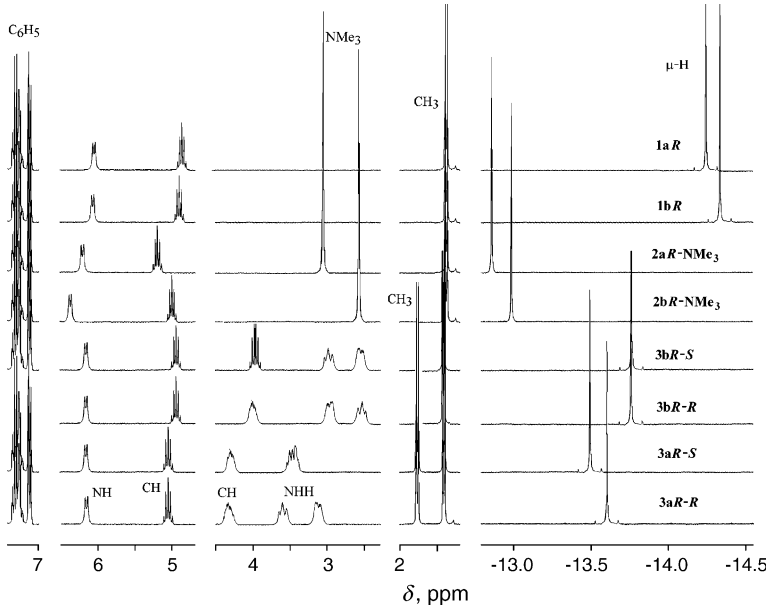

Figure 4. ^{1}H NMR spectra (250 MHz, $CDCl_3$, 25 °C) of the diastereomers [(μ-H)Os_3{μ-OCNH-(*R*)-CHMePh}$(CO)_{10}$] (*a*,*R*)-**1**, (*b*,*R*)-**1** and their derivatives with NMe_3 (*a*,*R*)-**2-NMe$_3$**, (*b*,*R*)-**2-NMe$_3$**, and (*R*)- or (*S*)-NH_2CHMePh (*a*,*R*,*R*)-**3**, (*b*,*R*,*R*)-**3**, (*a*,*R*,*S*)-**3**, and (*b*,*R*,*S*)-**3**.

(*b*,*R*)-**1** do not differ much allowing no differentiation of their signals in the aliphatic region. In general, the region between 1 and 8 ppm is hardly applicable to NMR analysis, in particular if we want to estimate the relative content of the diastereomers within a pair, during any reaction with their participation or in another solution. In addition, unpredictable overlapping of spectra may arise due to the NH signals being sensitive to medium acidity, temperature, overall concentration of hydrogen-bond donors/acceptors, etc.

The upfield region ($\delta < 0$), where only sharp single μ-H-resonances are present, is much more convenient from this point of view. These signals are sensitive positionally to the structure of the complexes and to the type of terminally bonded amine, and it can be seen from Figure 4 and Tables 1 and 2 that $\Delta\delta_{\mu\text{-H}}$ differences (in $CDCl_3$) for diastereomeric pairs **1**–**3** are quite appreciable (~0.1 ppm), except for the pair (*b*,*R*,*R*)-**3**/(*b*,*R*,*S*)-**3** ($\Delta\delta_{\mu\text{-H}} = 0.003$ ppm). The diastereomers **2** and **3** (*a*,*R*)-**2-NMe$_3$**/(*b*,*R*)-**2-NMe$_3$**, (*a*,*R*,*R*)-**3**/(*b*,*R*,*R*)-**3**, and (*a*,*R*,*S*)-**3**/(*b*,*R*,*S*)-**3** that differ one from another in a cluster-fragment configuration *a* or *b* demonstrate the larger $\Delta\delta_{\mu\text{-H}}$ differences relative to the unsubstituted parent **1**. Obviously, a terminally coordinated amino ligand acts as a substituent arm, which has shifted the stereogenic element and, in addition, nonequal structural changes had occurred in diastereomeric molecules after replacement of CO by amine. Similar effect was observed earlier for the isomeric nicotinyl clusters $[Os_3(\mu\text{-H})\{\mu\text{-}(S)\text{-}NC_5H_3C_4H_7NMe\}(CO)_{10}]$.[10] A larger chemical shift difference ($\Delta\delta_{\mu\text{-H}} = 0.086$ ppm) was registered when the pyridine ring substituent is closer to the Os_3 ring than when it is more remote ($\Delta\delta_{\mu\text{-H}} = 0.007$ ppm). So, after consideration of the high-field metal-hydride region, our conclusions remain the same with only one exception. The μ-H chemical shift differences are even larger in the case of the chiral $NH_2CHMePh$ substituent (*a*,*R*,*R*)-**3**/(*b*,*R*,*R*)-**3** and (*a*,*R*,*S*)-**3**/(*b*,*R*,*S*)-**3** than those for (*a*,*R*)-**2-NMe$_3$**/(*b*,*R*)-**2-NMe$_3$**. In this regard, complexes containing chiral amino substituent possess an advantage over those containing achiral amino ligands that the sufficient separation between hydride signals may allow their assignments and estimation of their relative quantity.

In order to clarify how sensitive are the $\Delta\delta_{\mu\text{-H}}$ magnitudes to the nature of solvent, and whether comparative μ-H-signal positions are maintained in going from one solvent to another the NMR behavior of the complexes **1**–**3** was studied in a number of common solvents (CD_3OD, C_6D_6, CD_3COCD_3 etc.). Table 1 and Figure 5 show the spectral media-specific changes for the diastereomers **1**–**3**.

First of all, one can see three spaced at ~0.7 ppm separate sets of μ-H resonances arising from the complexes **1**, **2**, and **3** that makes possible assigning the compounds with terminal CO, NMe_3, or $NH_2CHMePh$ substituents. Replacement of the CO ligand in the parent clusters (*a*,*R*)-**1**, (*b*,*R*)-**1** by an amino ligand resulted in a downfield shift of their μ-H singlets, with the hydride resonances for the NMe_3-substituted complexes **2** being shifted most. The downfield shift is an often-observed consequence of equatorial substitution at one of the bridgehead Os atoms in a hydrido-carbonyl double-bridged Os_3 cluster. For example, we may compare the reported chemical shifts $\delta_{\mu\text{-H}}$ −15.10 (in $CDCl_3$) and −14.71 (in CD_2Cl_2) for $[(\mu\text{-H})Os_3(\mu\text{-}1,2\text{-}\eta^2\text{-}C_7H_5N_2)(CO)_{10}]$[11] and $[(\mu\text{-H})Os_3(\mu\text{-}1,2\text{-}\eta^2\text{-}C_7H_5N_2)(CO)_9(PPh_3)]$,[11] respectively; $\delta_{\mu\text{-H}}$ −12.75, −12.65, and −12.3 (in $CDCl_3$) for $[(\mu\text{-H})Os_3(\mu\text{-OH})(CO)_{10}]$ and its derivatives with equatorial substituents PMe_2Ph[12] and $SMe(Bu^t)$,[13] respectively. Though this might not be always so. For example, the equatorially NMe_3-substituted 2-acylpyrrolyl cluster $[(\mu\text{-H})Os_3(\mu\text{-}COC_4H_3NH)(CO)_9(NMe_3)]$ was reported to give the μ-H signal at −14.35 ppm (in CD_2Cl_2)[14] while the same signal in the parent $[(\mu\text{-H})Os_3(\mu\text{-}COC_4H_3NH)(CO)_{10}]$ was observed at −13.0 ppm (in $CDCl_3$).[15]

As regards the NMe_3-substituted complexes, consideration of the available literature NMR data shows that an NMe_3 ligand equatorially bonded to one of the bridgehead osmium atoms has led to significant deshielding of μ-H nucleus with respect to other type of ligands located similarly in related clusters, just as with the row **1**–**3**. For example, while μ-H signals of complexes $[(\mu\text{-H})Os_3(\mu\text{-Cl})(CO)_{10}]$ and $[(\mu\text{-H})Os_3(\mu\text{-Cl})(CO)_9P(OMe)_3]$ were observed at −14.16 ppm (in $CDCl_3$)[16] and −14.24 ppm (in CD_2Cl_2),[17] respectively, the $\delta_{\mu\text{-H}}$ value for the NMe_3-substituted complex $[(\mu\text{-H})Os_3(\mu\text{-Cl})(CO)_9(NMe_3)]$ was found to be equal to −11.81 ppm (in CD_2Cl_2).[17] The pyridyl complexes $[(\mu\text{-H})Os_3(\mu\text{-}NC_5H_4)(CO)_{10}]$ and $[(\mu\text{-H})Os_3(\mu\text{-}NC_5H_4)(CO)_9(py)]$ were found[18] to display hydrido signals at −14.86 (in $CDCl_3$) and around −14.22 ppm (in $CDCl_3$), respectively, and the same signal was registered at −13.25 ppm (in CD_2Cl_2)[17] for $[(\mu\text{-H})Os_3(\mu\text{-}NC_5H_4)(CO)_9(NMe_3)]$. Presumably, with the literature cases above, larger μ-H deshielding for the NMe_3-substituted complexes **2** compared to the $NH_2CHMePh$-substituted complexes **3** could be best explained again by steric effects leading to a difference in angles between bonds but this is certainly not the whole explanation.

One can observe important regularities in a comparative location of μ-H signals for the diastereomeric pairs depending on both cluster fragment and ligand configurations. As it is evident from the spectra (Fig. 5), μ-H singlets from the complexes (*a*,*R*)-**1**, (*a*,*R*)-**2**, (*a*,*R*)-**3** having the *a* configuration of the cluster fragment (at given (*R*) configuration of the μ-carboxamido ligand) are always less shielded in comparison with the *b* configurational (*a*,*R*)-**1**, (*b*,*R*)-**2**, (*b*,*R*)-**3**, respectively. For the pair (*a*,*R*,*R*)-**3**/(*a*,*R*,*S*)-**3** having the same *a* cluster configuration and opposite-configurational terminal ligands, the hydride signal of the (*R*) substituted complex, (*a*,*R*,*R*)-**3**, appears to be shifted upfield (more shielded) relative to the (*S*) substituted complex, (*a*,*R*,*S*)-**3**, in all solvents. And vice versa, for the *b*-configurational pair (*b*,*R*,*R*)-**3**/(*b*,*R*,*S*)-**3**, the hydride signal for the (*R*) substituted complex (*b*,*R*,*R*)-**3** is seen always on the left (less shielded) relative to the (*S*) substituted complex (*b*,*R*,*S*)-**3**. Nothing can be said whether the same effect will be observed for other chiral amines as substituents or other

Table 1. IR (in C_6H_{12}), mass-spectral, ^{1}H NMR (250 MHz, in $CDCl_3$ relative to TMS, 25 °C) and ^{13}C NMR data (62.9 MHz, in C_6D_6 relative to TMS, 25 °C) for diastereomers [(μ-H)Os_3{μ-OCNH-(*R*)-CHMePh}$(CO)_9$L], where L = CO **1**, NMe_3 **2**, (*R*)- or (*S*)-NH_2CHMePh **3**

Complex	ν(CO) (cm^{-1})[a]	δ (ppm)[b]	Ion, m/z[c], I
(*a*,*R*)-**1**	2111w, 2065s, 2055s, 2020vs, 2010vs, 1992m, 1980w, 1959vw	^{1}H NMR: 7.30 (m, 5H, Ph), 6.05 (d, 1H, ^3J 7.0 Hz, NH), 4.97 (quint, 1H, ^3J 7.0 Hz, CH), 1.41 (d, 3H, ^3J 7.0 Hz, CH_3), −14.26 (s, 1H, μ-H); ^{13}C NMR: 184.520 (1C, *J* 2.3, 3.0, 6.7 Hz, μ-CO), 183.815 (1C, *J* 0.7 Hz, ax-CO at the top Os), 182.371 (1C, *J* 0.8 Hz, ax-CO at the top Os), 178.906 (1C, *J* 3.5 Hz, ax-CO at bridged OsC), 176.108 (1C, *J* 3.6 Hz, ax-CO at bridged OsO or eq-CO at bridged OsC), 176.051 (1C, *J* 3.1 Hz, eq-CO at a bridged OsC or ax-CO at bridged OsO), 175.749 (1C, *J* 0.0 Hz, eq-CO at the top Os), 175.734 (1C, *J* 13 Hz, *trans*-to-μ-H CO at bridged Os), 174.472 (1C, *J* 0.0 Hz, eq-CO at the top Os), 174.417 (1C, *J* 9.7 Hz, *trans*-to-μ-H CO at bridged Os), 173.664 (1C, *J* 3.6 Hz, eq-CO at bridged OsO).	M^+, 1005, 55; $[M-CO]^+$, 977, 31; $[M-(CO)_2]^+$, 949, 11; $[M-(CO)_3]^+$, 921, 28; $[M-(CO)_4]^+$, 893, 100; $[M-(CO)_5]^+$, 865, 100; $[M-(CO)_6]^+$, 837, 78; $[M-(CO)_7]^+$, 809, 82; $[M-(CO)_8]^+$, 781, 78; $[M-(CO)_9]^+$, 753, 78; $[M-(CO)_{10}]^+$, 725, 71; $[M-(CO)_{10}\ COH_2]^+$, 695, 82.
(*b*,*R*)-**1**	2107w, 2068s, 2057s, 2024vs, 2011vs, 1993m, 1979w, 1953vw	^{1}H NMR: 7.26 (m, 5H, Ph), 6.07 (d, 1H, ^3J 6.9 Hz, NH), 4.99 (quint, 1H, ^3J 6.9 Hz, CH), 1.38 (d, 3H, ^3J 6.9 Hz, CH_3), −14.36 (s, 1H, μ-H); ^{13}C NMR: 184.885 (1C, *J* 2.3, 3.0, 6.6 Hz, μ-CO), 184.355 (1C, *J* 0.7 Hz, ax-CO at the top Os), 182.303 (1C, *J* 0.7 Hz, ax-CO at the top Os), 178.870 (1C, *J* 3.5 Hz, ax-CO at bridged OsC), 175.986 (1C, *J* 3.1 Hz, ax-CO at bridged OsO or eq-CO at bridged OsC), 175.919 (1C, *J* 13.6 Hz, *trans*-to-μ-H CO at bridged Os), 175.610 (1C, *J* 3.4 Hz, eq-CO at a bridged OsC or ax-CO at bridged OsO), 175.421 (1C, *J* 0.0 Hz, eq-CO at the top Os), 174.596 (1C, *J* 10.1 Hz, *trans*-to-μ-H CO at bridged Os), 174.494 (1C, *J* 0.0 Hz, eq-CO at the top Os), 173.594 (1C, *J* 3.6 Hz, eq-CO at bridged OsO).	M^+, 1005, 42; $[M-CO]^+$, 977, 20; $[M-(CO)_2]^+$, 949, 10; $[M-(CO)_3]^+$, 921, 18; $[M-(CO)_4]^+$, 893, 70; $[M-(CO)_5]^+$, 865, 80; $[M-(CO)_6]^+$, 837, 78; $[M-(CO)_7]^+$, 809, 66; $[M-(CO)_8]^+$, 781, 68; $[M-(CO)_9]^+$, 753, 70; $[M-(CO)_{10}]^+$, 725, 68; $[M-(CO)_{10}COH_2]^+$, 695, 62.
(*a*,*R*)-**2**-NMe_3	2099m, 2054s, 2018s, 2008vs, 1994s, 1976w, 1974m, 1928m	^{1}H NMR: 7.33 (m, 5H, Ph), 6.21 (d, 1H, ^3J 7.3 Hz, NH), 5.20 (quint, 1H, ^3J 7.3 Hz, CH), 3.05 (s, 9H, NMe_3), 1.41 (d, 3H, ^3J 7.3 Hz, CH_3), −12.86 (s, 1H, μ-H); ^{13}C NMR: 187.0 (1C, *J* 3.2, 3.2, 6.4 Hz, μ-CO), 185.5 (1C, *J* ∼ 0 Hz, ax-CO at the top Os), 184.7 (1C, *J* 2.9 Hz, ax-CO at the bridged OsO), 182.1 (1C, *J* ∼ 0 Hz, ax-CO at the top Os), 180.0 (1C, *J* 3.7 Hz, CO at bridged Os), 178.7 (1C, *J* 11.2 Hz, *trans*-to-μ-H CO at bridged Os), 177.9 (1C, *J* 13.4 Hz, *trans*-to-μ-H CO at bridged Os), 175.0 (1C, *J* 4.0 Hz, CO at bridged Os), 174.2 (1C, *J* ∼ 0 Hz, eq-CO at the top Os), 173.7 (1C, *J* ∼ 0 Hz, eq-CO at the top Os), 141.3 −126.4 (6C, Ph), 58.0 (3C, *J* 138 Hz, $N(CH_3)_3$), 50.3 (1C, *J* 142 Hz, CH), 22.7 (1C, *J* 127 Hz, CH_3).	M^+, 1036, 0; $[M-Me]^+$, 1021, 55; $[M-C_3H_7]^+$, 993, 36; $[M-C_3H_7CO]^+$, 965, 9; $[M-C_3H_7(CO)_2]^+$, 937, 26; $[M-C_3H_7(CO)_3]^+$, 909, 98; $[M-C_3H_7(CO)_4]^+$, 881, 100; $[M-C_3H_7(CO)_5]^+$, 853, 87; $[M-C_3H_7(CO)_6]^+$, 825, 83; $[M-C_3H_7(CO)_7]^+$, 797, 79; $[M-C_3H_7(CO)_8]^+$, 769, 75; $[M-C_3H_7(CO)_9]^+$, 741, 62; $[M-NC_4H_9(CO)_9]^+$, 713, 96.
(*b*,*R*)-**2**-NMe_3	2089m, 2048s, 2015s, 2006vs, 1986s, 1974w, 1965m, 1926m	^{1}H NMR: 7.24 (m, 5H, Ph), 6.38 (d, 1H, ^3J 7.2 Hz, NH), 5.00 (quint, 1H, ^3J 7.2 Hz, CH), 2.53 (s, 9H, NMe_3), 1.42 (d, 3H, ^3J 7.2 Hz, CH_3), −12.99 (s, 1H, μ-H); ^{13}C NMR: 187.8 (1C, *J* 2.5, 3.7, 6.4 Hz, μ-CO), 185.9 (1C, *J* ∼ 0 Hz, ax-CO at the top Os), 184.8 (1C, *J* 2.8 Hz, ax-CO at the bridged OsO), 182.1 (1C, *J* ∼ 0 Hz, ax-CO at the top Os), 180.1 (1C, *J* 3.7 Hz, CO at bridged Os), 178.7 (1C, *J* 11.2 Hz, *trans*-to-μ-H CO at bridged Os), 178.2 (1C, *J* 13.5 Hz, *trans*-to-μ-H CO at bridged Os), 175.1 (1C, *J* 3.8 Hz, CO at bridged Os), 174.3 (1C, *J* ∼ 0 Hz, eq-CO at the top Os), 174.0 (1C, *J* ∼ 0 Hz, eq-CO at the top Os), 145.2 −125.6 (6C, Ph), 57.8 (3C, *J* 137 Hz, $N(CH_3)_3$), 51.5 (1C, *J* 143 Hz, CH), 22.3 (1C, *J* 129 Hz, CH_3).	M^+, 1036, 4; $[M-Me]^+$, 1021, 36; $[M-C_3H_7]^+$, 993, 20; $[M-C_3H_7CO]^+$, 965, 5; $[M-C_3H_7(CO)_2]^+$, 937, 19; $[M-C_3H_7(CO)_3]^+$, 909, 72; $[M-C_3H_7(CO)_4]^+$, 881, 82; $[M-C_3H_7(CO)_5]^+$, 853, 70; $[M-C_3H_7(CO)_6]^+$, 825, 61; $[M-C_3H_7(CO)_7]^+$, 797, 71; $[M-C_3H_7(CO)_8]^+$, 769, 71; $[M-C_3H_7(CO)_9]^+$, 741, 69; $[M-NC_4H_9(CO)_9]^+$, 713, 62.
(*a*,*R*,*R*)-**3**	2096m, 2047vs, 2013vs, 2003vs, 1991vs, 1975w, 1965m, 1927m	^{1}H NMR: 7.38 (m, 10H, 2Ph), 6.16 (d, 1H, ^3J 7.0 Hz, NH), 5.07 (quint, 1H, ^3J 7.0 Hz, CH), 4.35 (br m, 1H, CH), 3.58 (br dd, 1H, ^2J 11.5 Hz, ^3J 6.7 Hz, N*H*H), 3.13 (br dd, 1H, ^2J 11.5 Hz, ^3J 4.8 Hz, NH*H*), 1.75 (d, 3H, ^3J 6.7 Hz, CH_3), 1.39 (d, 3H, ^3J 7.0 Hz, CH_3), −13.58 (s, 1H, μ-H); ^{13}C NMR: 186.0 (1C, *J* 3.2, 3.2, 6.4 Hz, μ-CO), 185.4 (1C, *J* ∼ 0 Hz, ax-CO at the top Os), 184.6 (1C, *J* 2.9 Hz, ax-CO at bridged OsO), 182.1 (1C, *J* ∼ 0 Hz, ax-CO at the top Os), 179.8 (1C, *J* 4.0 Hz, CO at bridged Os), 179.5 (1C, *J* 11.3 Hz, *trans*-to-μ-H CO at bridged Os), 177.5 (1C, *J* 13.0 Hz, *trans*-to-μ-H CO at bridged Os), 175.1 (1C, *J* 3.8 Hz, CO at bridged Os), 174.5 (1C, *J* ∼ 0 Hz, eq-CO at the top Os), 174.4 (1C, *J* ∼ 0 Hz, eq-CO at the top Os), 144.8−125.3 (12C, 2Ph), 58.6 (1C, *J* 143 Hz, CH), 51.0 (1C, *J* 142 Hz, CH), 23.2 (1C, *J* 126 Hz, CH_3), 22.0 (1C, *J* 128 Hz, CH_3).	M^+, 1098, 0; $[M-Ph]^+$, 1021, 36; $[M-C_8H_9]^+$, 993, 60; $[M-C_8H_9CO]^+$, 965, 10; $[M-C_8H_9(CO)_2]^+$, 937, 24; $[M-C_8H_9(CO)_3]^+$, 909, 100; $[M-C_8H_9(CO)_4]^+$, 881, 94; $[M-C_8H_9(CO)_5]^+$, 853, 84; $[M-C_8H_9(CO)_6]^+$, 825, 76; $[M-C_8H_9(CO)_7]^+$, 797, 72; $[M-C_8H_9(CO)_8]^+$, 769, 72; $[M-C_8H_9(CO)_9]^+$, 741, 62; $[M-NC_9H_{11}(CO)_9]^+$, 713, 88.
(*a*,*R*,*S*)-**3**	2095m, 2049vs, 2013vs, 2003vs, 1993vs, 1976w, 1965m, 1929m	^{1}H NMR: 7.39 (m, 10H, 2Ph), 6.19 (d, 1H, ^3J 7.4 Hz, NH), 5.06 (quint, 1H, ^3J 7.0 Hz, CH), 4.29 (br m, 1H, CH), 3.46 (m, 2H, ^2J 9.6 Hz, ^3J 6.7 Hz, N*HH*), 1.76 (d, 3H, ^3J 6.7 Hz, CH_3), 1.37 (d, 3H, ^3J 6.7 Hz, CH_3), −13.49 (s, 1H, μ-H); ^{13}C NMR: 185.9 (1C, *J* 3.2, 3.2, 6.4 Hz, μ-CO), 185.5 (1C, *J* ∼ 0 Hz, ax-CO at the top Os), 185.1 (1C, *J* 2.8 Hz, ax-CO at bridged OsO), 182.3 (1C, *J* ∼ 0 Hz, ax-CO at the top Os), 179.6 (1C, *J* 3.9 Hz, CO at bridged Os), 179.0 (1C, *J* 11.2 Hz, *trans*-to-μ-H CO at bridged Os), 177.7 (1C, *J* 13.0 Hz, *trans*-to-μ-H CO at bridged Os), 175.2 (1C, *J* 3.8 Hz, CO at bridged Os), 174.5 (1C, *J* ∼ 0 Hz, eq-CO at the top Os), 174.48 (1C, *J* ∼ 0 Hz, eq-CO at the top Os), 143.9−125.9 (12C, 2Ph), 61.4 (1C, *J* 141 Hz, CH), 50.3 (1C, *J* 143 Hz, CH), 21.6 (1C, *J* 126 Hz, CH_3), 21.4 (1C, *J* 127 Hz, CH_3).	M^+, 1098, 0; $[M-Ph]^+$, 1021, 31; $[M-C_8H_9]^+$, 993, 23; $[M-C_8H_9CO]^+$, 965, 7; $[M-C_8H_9(CO)_2]^+$, 937, 20; $[M-C_8H_9(CO)_3]^+$, 909, 81; $[M-C_8H_9(CO)_4]^+$, 881, 98; $[M-C_8H_9(CO)_5]^+$, 853, 74; $[M-C_8H_9(CO)_6]^+$, 825, 72; $[M-C_8H_9(CO)_7]^+$, 797, 71; $[M-C_8H_9(CO)_8]^+$, 769, 72; $[M-C_8H_9(CO)_9]^+$, 741, 70; $[M-NC_9H_{11}(CO)_9]^+$, 713, 100.

(*b*,*R*,*R*)-**3**	2094m, 2050vs, 2013vs, 2005vs, 1994vs, 1975w, 1965m, 1929m	^{1}H NMR: 7.25 (m, 10H, 2Ph), 6.32 (d, 1H, ^3J 6.6 Hz, NH), 4.93 (quint, 1H, ^3J 6.9 Hz, CH), 4.01 (br m, 1H, CH), 2.97 (br dd, 1H, ^2J 11.3 Hz, ^3J 3.8 Hz, N*H*H), 2.53 (br dd, 1H, ^2J 9.9 Hz, ^3J 4.9 Hz, NH*H*), 1.38 (2d, 6H, ^3J 6.7 Hz, 2CH$_3$), −13.76 (s, 1H, μ-H); ^{13}C NMR: 186.6 (1C, *J* 2.6, 3.8, 6.4 Hz, μ-CO), 185.9 (1C, *J* ∼ 0 Hz, ax-CO at the top Os), 184.9 (1C, *J* 2.9 Hz, ax-CO at bridged OsO), 182.1 (1C, *J* ∼ 0 Hz, ax-CO at the top Os), 179.7 (1C, *J* 4.0 Hz, CO at bridged Os), 179.3 (1C, *J* 11.3 Hz, *trans*-to-μ-H CO at bridged Os), 177.8 (1C, *J* 13.1 Hz, *trans*-to-μ-H CO at bridged Os), 175.1 (1C, *J* 3.8 Hz, CO at bridged Os), 174.6 (1C, *J* ∼ 0 Hz, eq-CO at the top Os), 174.5 (1C, *J* ∼ 0 Hz, eq-CO at the top Os), 144.6–125.2 (12C, 2Ph), 60.9 (1C, *J* 142 Hz, CH), 50.9 (1C, *J* 140 Hz, CH), 22.1 (1C, *J* 128 Hz, CH$_3$), 21.9 (1C, *J* 129 Hz, CH$_3$).	M$^+$, 1098, 0; [M−Ph]$^+$, 1021, 77; [M−C$_8$H$_9$]$^+$, 993, 31; [M−C$_8$H$_9$CO]$^+$, 965, 12; [M−C$_8$H$_9$(CO)$_2$]$^+$, 937, 28; [M−C$_8$H$_9$(CO)$_3$]$^+$, 909, 100; [M−C$_8$H$_9$(CO)$_4$]$^+$, 881, 95; [M−C$_8$H$_9$(CO)$_5$]$^+$, 853, 73; [M−C$_8$H$_9$(CO)$_6$]$^+$, 825, 72; [M−C$_8$H$_9$(CO)$_7$]$^+$, 797, 71; [M−C$_8$H$_9$(CO)$_8$]$^+$, 769, 70; [M−C$_8$H$_9$(CO)$_9$]$^+$, 741, 61; [M−NC$_9$H$_{11}$(CO)$_9$]$^+$, 713, 81.
(*b*,*R*,*S*)-**3**	2095m, 2048vs, 2014vs, 2005vs, 1994vs, 1974w, 1966m, 1928m	^{1}H NMR: 7.25 (m, 10H, 2Ph), 6.33 (d, 1H, ^3J 6.5 Hz, NH), 4.91 (quint, 1H, ^3J 6.5 Hz, CH), 3.99 (sext, 1H, CH), 2.96 (br dd, 1H, ^3J 7.1 Hz, N*H*H), 2.53 (br dd, 1H, ^2J 11.3 Hz, ^3J 4.9 Hz, NH*H*), 1.40 (2d, 6H, ^3J 6.5 Hz, 2CH$_3$), −13.76 (s, 1H, μ-H); ^{13}C NMR: 186.5 (1C, *J* 3.7, 4.0, 6.4 Hz, μ-CO), 185.8 (1C, *J* ∼ 0 Hz, ax-CO at the top Os), 184.6 (1C, *J* 2.9 Hz, ax-CO at bridged OsO), 182.1 (1C, *J* ∼ 0 Hz, ax-CO at the top Os), 179.9 (1C, *J* 4.0 Hz, CO at bridged Os), 179.2 (1C, *J* 11.3 Hz, *trans*-to-μ-H CO at bridged Os), 177.8 (1C, *J* 13.1 Hz, *trans*-to-μ-H CO at bridged Os), 175.2 (1C, *J* 3.8 Hz, CO at bridged Os), 174.7 (1C, *J* ∼ 0 Hz, eq-CO at the top Os), 174.5 (1C, *J* ∼ 0 Hz, eq-CO at the top Os), 143.0–126.1 (12C, 2Ph), 59.7 (1C, *J* 141 Hz, CH), 50.4 (1C, *J* 140 Hz, CH), 22.5 (1C, *J* 129 Hz, CH$_3$), 21.2 (1C, *J* 127 Hz, CH$_3$).	M$^+$, 1098, 0; [M−Ph]$^+$, 1021, 71; [M−C$_8$H$_9$]$^+$, 993, 30; [M−C$_8$H$_9$CO]$^+$, 965, 11; [M−C$_8$H$_9$(CO)$_2$]$^+$, 937, 28; [M−C$_8$H$_9$(CO)$_3$]$^+$, 909, 101; [M−C$_8$H$_9$(CO)$_4$]$^+$, 881, 94; [M−C$_8$H$_9$(CO)$_5$]$^+$, 853, 74; [M−C$_8$H$_9$(CO)$_6$]$^+$, 825, 71; [M−C$_8$H$_9$(CO)$_7$]$^+$, 797, 73; [M−C$_8$H$_9$(CO)$_8$]$^+$, 769, 68; [M−C$_8$H$_9$(CO)$_9$]$^+$, 741, 60; [M−NC$_9$H$_{11}$(CO)$_9$]$^+$, 713, 100.

[a] vs, Very strong; s, strong; m, medium; w, weak; vw, very weak.
[b] While C-1, *ortho*-, *meta*- and *para*-carbons of Ph groups have ^{13}C NMR discrete sharp signals their joint intervals are given because of space limitations.
[c] Refers to ^{192}Os.

chiral bridging ligands. The magnitudes of $\Delta\delta_{\mu\text{-H}}$ for (*a*)-**3** or (*b*)-**3** pairs with identical cluster-fragment configurations are mainly quite large ($\Delta\delta_{\mu\text{-H}}$ for less chemically stable (*a*)-**3** is higher than for (*b*)-**3**) and sometimes mount to 0.17 ppm but they are smaller than those for the mentioned above *a*/*b*-configurational pairs.

It is evident from Figure 5 and Table 2 that the $\Delta\delta_{\mu\text{-H}}$ value for every diastereomeric pair depends significantly on the nature of solvent. For example, for pairs (*a*,*R*)-**1**/(*b*,*R*)-**1** (entries 1, 2) and (*a*,*R*)-**2-NMe$_3$**/(*b*,*R*)-**2-NMe$_3$** (Table 2, entries 3, 4), μ-H signals are spaced at 0.02–0.03 ppm in benzene solution, while in CCl_4 or $CDCl_3$ solutions this distance is approximately 4-fold higher (0.10–0.13 ppm). The similar solvent-specific behavior is also observed for the *a*/*b* pairs of **3** (entries 9, 10 and 11, 12), but chiral substituents result other proportions so that approximately 18-fold increase of the $\Delta\delta_{\mu\text{-H}}$ value is observed for (*a*,*R*,*R*)-**3**/(*b*,*R*,*R*)-**3** (from 0.010 to 0.179 ppm) and only 1.5-fold increase is observed for (*a*,*R*,*S*)-**3**/(*b*,*R*,*S*)-**3** (from 0.264 to 0.362 ppm) in going from benzene to $CDCl_3$. In contrast to the *a*/*b* pairs, diastereomeric peak separation for the pairs (*a*,*R*,*R*)-**3**/(*a*,*R*,*S*)-**3** (entries 5, 6) and (*b*,*R*,*R*)-**3**/(*b*,*R*,*S*)-**3** (entries 7, 8) is largest in benzene (0.167 and 0.062 ppm).

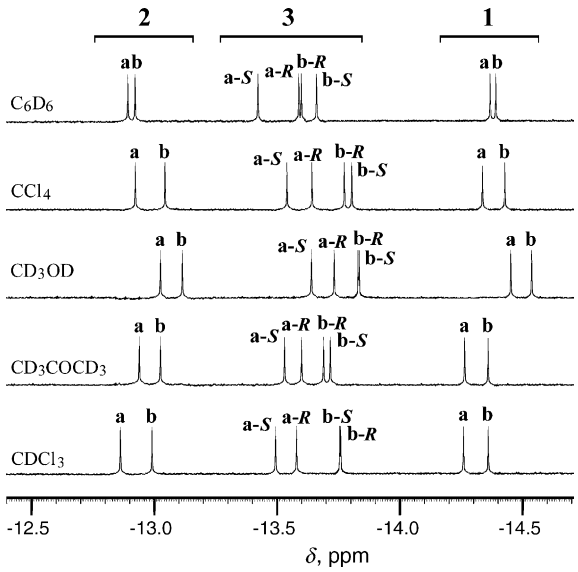

Figure 5. The upfield region of ^{1}H NMR spectra of the diastereomers **1**–**3** in various solvents (250 MHz, 25 °C). Due to space limitations, index ***R*** mentioning the (*R*) configuration of μ-ligand is omitted after *a* or *b*.

3. Conclusions

Eight related complexes [(μ-H)Os$_3${μ-OCNH-(*R*)-CHMePh}(CO)$_9$L] {L = CO **1**, NMe$_3$ **2**, and (*S*)-(−)- or (*R*)-(+)-NH$_2$CHMePh **3**}, containing two or three stereogenic centers were prepared and their physicochemical properties were investigated comparing with each other. With respect to IR and specific rotation determinations, ^{1}H NMR spectroscopy in hydride region is the highly informative method allowing to detect

Table 2. ^{1}H NMR chemical shift nonequivalencies for the diastereomers **1**–**3** in various solvents

Entry	Complex	$\lvert\Delta\delta_{\mu\text{-H}}\rvert \pm 0.001$ ppm*				
		$CDCl_3$	$(CD_3)_2CO$	CCl_4	C_6D_6	CD_3OD
1	(*a*,*R*)-**1**	0.100	0.095	0.091	0.023	0.085
2	(*b*,*R*)-**1**					
3	(*a*,*R*)-**2-NMe$_3$**	0.129	0.086	0.121	0.030	0.089
4	(*b*,*R*)-**2-NMe$_3$**					
5	(*a*,*R*,*R*)-**3**	0.086	0.069	0.102	0.167	0.093
6	(*a*,*R*,*S*)-**3**					
7	(*b*,*R*,*R*)-**3**	0.003	0.028	0.029	0.062	0.004
8	(*b*,*R*,*S*)-**3**					
9	(*a*,*R*,*R*)-**3**	0.179	0.089	0.133	0.010	0.098
10	(*b*,*R*,*R*)-**3**					
11	(*a*,*R*,*S*)-**3**	0.362	0.186	0.264	0.239	0.195
12	(*b*,*R*,*S*)-**3**					

*The $\lvert\Delta\delta_{\mu\text{-H}}\rvert$ values are average from 5 to 6 independent measurements, with strictly identical conditions being not kept, but for all that, statistical error did not exceed ±0.001 ppm.

inherent tiny differences between the diastereomers. The relative values of $\delta_{\mu\text{-H}}$ for corresponding diastereomers depend on a number of stereogenic centers in the molecule, the nature of L (CO or amine) and solvent and most of all on the absolute configuration of the cluster fragment [HOs_3(μ-OCN)]. It was shown that μ-H signals occupy the certain relative positions in ^{1}H NMR spectra in compliance with the specific cluster-fragment configuration (*a* or *b*). The molecules having the *b* configuration of the cluster fragment and arranged in space as the structurally characterized and depicted in Figure 3 complex (+)-[(μ-H)Os_3{μ-OCNH-(*R*)-CHMePh}$(CO)_{10}$] (*b*)-**1** display always the higher-field μ-H signal in comparison with the opposite-configurational species *a*. Thus, analytical NMR spectroscopy makes it possible to recognize the absolute configuration of diastereomer and really to know what is the outcome of a specific asymmetric reaction with its participation. We suppose that similar correlations exist with other carboxamido complexes, having specifically no chirality on the bridging ligand, but having chiral terminally bonded ligand. The study showed that chirality of the amino substituent favors the more significant spectroscopic differentiation, $\Delta\delta_{\mu\text{-H}}$, between diastereomers, especially if the chlorinated hydrocarbons ($CDCl_3$, CCl_4) are used as solvents, and then $\Delta\delta_{\mu\text{-H}}$ may achieve the significant values (0.36 ppm for the diastereomers [(μ-H)Os_3{μ-OCNH-(*R*)-CHMePh}$(CO)_9${(*S*)-NH_2CHMePh}] (*a*,*R*,*S*)-**3**/(*b*,*R*,*S*)-**3** in $CDCl_3$) allowing quantitative measuring of the diastereomeric proportion.

The $\Delta\delta_{\mu\text{-H}}$ values for the diastereomeric pairs having identical configuration of the cluster fragment *a* or *b* but different (*R*) or (*S*) configurations of amino substituent (NH_2CHMePh) is smaller in general than those for the above mentioned pairs having different configuration of the cluster fragment but the same chiral amino substituent. Depending strongly on the nature of solvent, the $\Delta\delta_{\mu\text{-H}}$ values range from 0.07 to 0.10 for the *a* pair and from 0.003 to 0.06 for the *b* pair. Availability of obtained empirical correlations between NMR chemical shift difference, $\Delta\delta_{\mu\text{-H}}$, and the nature of solvent should allow examining optically active complexes like (*a*)-**1** or (*b*)-**1** as chiral reagents suitable for determining enantiomer composition and absolute configuration of NH_2CHMePh and, probably, of other amines.

4. Experimental

4.1. General

^{1}H NMR spectra were recorded on a Bruker DPX-250 spectrometer, and were referenced to internal Me_4Si. IR spectra were obtained using a Specord 75-IR spectrometer with 0.2 mm CaF_2 cells. Mass spectra were obtained on a MX-1310 mass spectrometer at 60 eV. Optical rotations were measured on a 'Jasco DIP-360' polarimeter.

(*R*)-(−)-1-phenylethylamine (Merck; GC-analytical purity >99%; $[\alpha]_D^{20} = +37$ to +39) was used for synthesis without purification. (+)- and (−)-Rotating stereoisomers of 1,1,1,2,2,2,3,3,3,3-decacarbonyl-1,2-μ-hydrido-1,2-μ-(1-phenylethylaminocarbonyl)*triangulo*-triosmium, (*b*)-**1**, and (*a*)-**1**, respectively were synthesized as described in our preliminary communication[6] from the labile complex [$Os_3(CO)_{11}$NCMe], which was in turn prepared by the literature method from [$Os_3(CO)_{12}$].[19]

4.2. 1,1,1,2,2,3,3,3,3,3-Nonacarbonyl-1,2-μ-hydrido-2-trimethylamine-1,2-μ-[(*R*)-1-phenylethylaminocarbonyl)]-*triangulo*-triosmium, (*a*,*R*)-2-NMe$_3$

A mixture of (−)-[(μ-H)Os_3{μ-OCNH-(*R*)-CHMePh}-$(CO)_{10}$] (*a*,*R*)-**1** (47 mg, 4.7×10^{-5} mol) in diethyl ether (10 mL) and solid $Me_3NO{\cdot}2H_2O$ (5.5 mg, 5×10^{-5} mol) was stirred in a hermetic vessel overnight. The reaction solution has changed its initially yellow color to orange. Chromatography on thin-layer silica plates using hexane–diethyl ether (5:7) as eluent showed orange band of the product (*a*,*R*)-**2-NMe$_3$**, which was extracted with diethyl ether followed by treatment of extract with dry hexane and pentane (2 and 10 mL, respectively) and

removal of volatile components under reduced pressure (water pump). The yield of the orange polycrystalline (*a*,*R*)-**2-NMe$_3$** is 94% (45.5 mg, 4.4×10^{-5} mol). $[\alpha]_D^{20}=+3$ (*c* 1, $CHCl_3$). IR, mass-spectral and ^1H and ^{13}C NMR data in Table 1.

4.3. 1,1,1,2,2,3,3,3,3-Nonacarbonyl-1,2-μ-hydrido-2-trimethylamine-1,2-μ-[(*R*)-1-phenylethylaminocarbonyl)]-*triangulo*-triosmium, (*b*,*R*)-2-NMe$_3$

Compound (+)-[(μ-H)Os_3{μ-OCNH-(*R*)-CHMePh}-$(CO)_{10}$] (*b*,*R*)-**1** (45 mg, 4.5×10^{-5} mol) was allowed to react with $Me_3NO{\cdot}2HO$(5.3 mg, 4.8×10^{-5} mol) in diethyl ether (10 mL) at room temperature for a night. Removal of volatile components from the resulted orange reaction mixture has afforded orange powder of the product (*b*,*R*)-**2-NMe$_3$** (41.3 mg, 4.0×10^{-5} mol). $[\alpha]_D^{20}=+45$ (*c* 1, $CHCl_3$). IR, mass-spectral and ^1H and ^{13}C NMR data in Table 1.

4.4. 1,1,1,2,2,3,3,3,3-Nonacarbonyl-1,2-μ-hydrido-2-(*R*)-1-phenylethylamine-1,2-μ-[(*R*)-1-phenylethylaminocarbonyl)]*triangulo*-triosmium, (*a*,*R*,*R*)-3

To the stirred solution of (−)-[(μ-H)Os_3{μ-OCNH-(*R*)-CHMePh}$(CO)_{10}$] (*a*,*R*)-**1** (~40 mg, 4×10^{-5} mol) in THF (2 mL) containing also (*R*)-(+)-NH_2CHMePh (34 mg, 2.8×10^{-4} mol), $Me_3NO{\cdot}2H_2O$ (5.1 mg, 4.6×10^{-4} mol) in methanol (0.5 mL) was added in drops for 10 min. After about 2 h, the resulting yellow solution was concentrated to 2–3 mL, diluted with 2 mL hexane and chromatographed on thin-layer silica plates with hexane–diethyl ether (2:1) as eluent. The main band of the diastereomer (−)-[(μ-H)Os_3{μ-OCNH-(*R*)-CHMePh}-$(CO)_9${(*R*)-NH_2CHMePh)}] (*a*,*R*,*R*)-**3** was extracted by diethyl ether (three times by about 4–5 mL) on a glass filter. To the resulted filtrate, 2 mL dry hexane and 10 mL dry pentane were added to minimize the loss of the volatile complex (*a*,*R*,*R*)-**3** under pumping, and solvents were then pumped out until dry without warming. Additional treatment of an oily residue with 2 mL dry pentane and repeated pumping gave (*a*,*R*,*R*)-**3** as orange-yellow solid in yield 69% (30.3 mg, 2.8×10^{-5} mol). $[\alpha]_D^{20}=-6$ (*c* 1, $CHCl_3$). IR, mass-spectral and ^1H and ^{13}C NMR data in Table 1.

4.5. 1,1,1,2,2,3,3,3,3-Nonacarbonyl-1,2-μ-hydrido-2-(*R*)-1-phenylethylamine-1,2-μ-[(*R*)-1-phenylethylaminocarbonyl)]*triangulo*-triosmium, (*b*,*R*,*R*)-3

To the stirred solution of (+)-[(μ-H)Os_3{μ-OCNH-(*R*)-CHMePh}$(CO)_{10}$] (*b*,*R*)-**1** (62 mg, 6.2×10^{-5} mol) in THF (3 mL) containing also (*R*)-(+)-NH_2CHMePh (87 mg, 7.2×10^{-4} mol), $Me_3NO{\cdot}2H_2O$ (7.4 mg, 6.7×10^{-5} mol) in methanol (0.5 mL) was added in drops for 10 min. After about 2 h, the resulting solution was concentrated to 2–3 mL, diluted with 2 mL hexane and chromatographed on thin-layer silica plates with hexane–diethyl ether (2:1) as eluent. The main band of the diastereomer (+)-[(μ-H)Os_3{μ-OCNH-(*R*)-CHMePh}-$(CO)_9${(*R*)-NH_2CHMePh)}] (*b*,*R*,*R*)-**3** was extracted by diethyl ether, filtered, and then dry hexane (2 mL) and dry pentane (10 mL) were added to the resulted mixture. Solvents were then pumped out under vacuum of a water pump without vessel warming, an oily residue was treated with dry pentane (2 mL) and repeatedly pumped out until dry. The complex (*b*,*R*,*R*)-**3** was isolated as orange-yellow solid in yield about 73% (49.7 mg, 4.6×10^{-5} mol). $[\alpha]_D^{20}=+69$ (*c* 1, $CHCl_3$). IR, mass-spectral and ^1H and ^{13}C NMR data in Table 1.

4.6. 1,1,1,2,2,3,3,3,3-Nonacarbonyl-1,2-μ-hydrido-2-(*S*)-1-phenylethylamine-1,2-μ-[(*R*)-1-phenylethylaminocarbonyl)]*triangulo*-triosmium, (*a*,*R*,*S*)-3

Synthesis of (−)-[(μ-H)Os_3{μ-OCNH-(*R*)-CHMePh}-$(CO)_9${(*S*)-NH_2CHMePh)}] (*a*,*R*,*S*)-**3** from (*a*,*R*)-**1** (56.6 mg, 5.7×10^{-5} mol) and (*S*)-(−)-NH_2 CHMePh (29.7 mg, 2.5×10^{-4} mol) in the presence of $Me_3NO{\cdot}2H_2O$ (6.7 mg, 6.7×10^{-5} mol) was carried out in a similar manner as for (*a*,*R*,*R*)-**3** (Section 4.4) and affords the yellow complex (*a*,*R*,*S*)-**3** (the yield is 72%, 45 mg, 4.1×10^5 mol). $[\alpha]_D^{20}=-17$ (*c* 1, $CHCl_3$). IR, mass-spectral and ^1H and ^{13}C NMR data in Table 1.

4.7. 1,1,1,2,2,3,3,3,3-Nonacarbonyl-1,2-μ-hydrido-2-(*S*)-1-phenylethylamine-1,2-μ-[(*R*)-1-phenylethylaminocarbonyl)]*triangulo*-triosmium, (*b*,*R*,*S*)-3

Stereoisomer (+)-[(μ-H)Os_3{-OCNH-(*R*)-CHMePh}-$(CO)_9$ {(*S*)-NH_2CHMePh)}] (*b*,*R*,*S*)-**3** as yellow solid was prepared from (+)-[(μ-H)Os_3{μ-OCNH-(*R*)-CHMePh}$(CO)_{10}$] (*b*,*R*)-**1** (56.4 mg, 5.6×10^{-5} mol) and (*S*)-(−)-NH_2CHMePh (35 mg, 2.9×10^{-4} mol) in the presence of $Me_3NO{\cdot}2H_2O$ (7 mg, 6.3×10^{-5} mol) according to the procedure for (*b*,*R*,*R*)-**3** (Section 4.5) in yield 91% (55.6 mg, 5.1×10^{-5} mol). $[\alpha]_D^{20}=+59$ (*c* 1, $CHCl_3$). IR, mass-spectral and ^1H and ^{13}C NMR data in Table 1.

Acknowledgements

We thank the Russian Foundation for Basic Research for funding of this work (grants 01-03-32426 and 03-03-06628).

References and Notes

1. Arce, A. J.; Deeming, A. J. *Chem. Commun.* **1980**, 1102.
2. Maksakov, V. A.; Ershova, V. A.; Kirin, V. P.; Golovaneva, I. F.; Michaylova, A. Ya.; Klyagina, A. P. *Dokl. Akad. Nauk SSSR (Russ.)* **1988**, *299*, 1142.
3. Ershova, V. A.; Tkachev, S. V.; Golovin, A. V.; Al't, L. Ya *Mendeleev Commun.* **1998**, 208.
4. Ershova, V. A.; Golovin, A. V.; Pogrebnyak, V. M. *J. Organomet. Chem.* **2002**, *658*, 147.
5. Ershova, V. A.; Virovets, A. V.; Golovin, A. V.; Pogrebnyak, V. M. *Inorg. Chem. Commun.* **2002**, *5*, 963.

6. Vega, A.; Spodine, E.; Arce, A.; Manzur, J.; Garcia, A. M.; Garland, M. T. *Acta Crystallogr., Sect. C: Cryst. Struct. Commun.* **1999**, *55*, 322.
7. Maksakov, V. A.; Ershova, V. A.; Virovets, V. A.; Podberezskaya, N. V.; Semyannikov, P. P.; Buyanovskaya, A. G. *Metalloorg. Khim. (Russ.)* **1993**, *6*, 231.
8. Maksakov, V. A.; Ershova, V. A.; Virovets, A. V.; Slovokhotov, Yu. L.; Podberezskaya, N. V.; Struchkov, Yu. T. *Metalloorg. Khim. (Russ.)* **1991**, *4*, 305.
9. Clarke, L. P.; Raithby, P. R.; Shields, G. P. *Polyhedron* **1997**, *16*, 3775.
10. Deeming, A. J.; Stchedro, M. J.; Whittaker, C.; Arce, A. J.; De Sanctis, Y.; Steed, J. W. *J. Chem. Soc., Dalton trans*. **1999**, 3289.
11. Akther, J.; Azam, K. A.; Das, A. R.; Hursthouse, M. B.; Kabir, S. E.; Malik, K. M. A.; Rosenberg, E.; Tesmer, M.; Vahrenkamp, H. *J. Organomet. Chem.* **1999**, *588*, 211.
12. Deeming, A. J.; Manning, P. J.; Rothwell, I. P.; Hursthouse, M. B.; Walker, N. P. C. *J. Chem Soc., Dalton trans*. **1984**, 2039.
13. Kiriakidou-Kazemifar, N. K.; Kretzschmar, E.; Carlsson, H.; Monari, M.; Selva, S.; Nordlander, E. *J. Organomet. Chem.* **2001**, *623*, 191.
14. Clarke, L. P.; Raithby, P. R.; Shields, G. P. *Polyhedron* **1997**, *16*, 3775.
15. Arce, A. J.; De Sanctis, Y.; Deeming, A. J. *J. Organomet. Chem.* **1986**, *311*, 371.
16. Deeming, A. J.; Hasso, S. *J. Organomet. Chem.* **1976**, *114*, 313.
17. Ditzel, E. J.; Hanson, B. E.; Johnson, B. F. G.; Lewis, J. *J. Chem. Soc., Dalton trans*. **1987**, 1285.
18. Yin, C. C.; Deeming, A. J. *J. Chem. Soc., Dalton trans*. **1975**, 2091.
19. Johnson, B. F. G.; Lewis, J.; Pippard, D. *J. Chem. Soc., Dalton trans*. **1981**, 407.